Evolution of a Middle Jurassic back-arc basin, Cedros Island, Baja California: Evidence from a marine volcaniclastic apron

CATHY J. BUSBY-SPERA *Department of Geological Sciences, University of California, Santa Barbara, California 93106*

ABSTRACT

A rifted arc-ophiolite assemblage and overlying volcaniclastic rocks, all of late Middle Jurassic age, represent a fragment of the frontal-arc margin of a back-arc basin, now exposed on Cedros Island in Baja California (Mexico). Ophiolite generation was immediately followed by progradation of a deep-marine volcaniclastic apron (Gran Cañon Formation) contemporaneous with the growth of island-arc volcanoes. This back-arc apron shows relatively simple, uniform sedimentation patterns that may be recognizable in other back-arc basins isolated from terrigenous sediment influx.

The progradational back-arc apron sequence includes, from base to top, (1) the tuff lithofacies—thin-bedded, well-sorted, laterally continuous tuffs that thicken into basement paleo-lows. These were deposited from dilute sediment gravity flows generated by eruptions from a deeply submerged, nascent arc. (2) the lapilli tuff-tuff breccia lithofacies—medium- to very thick-bedded lapilli tuffs and tuff breccias. These were deposited from debris flows on proximal parts of the apron, and high-density turbidites were deposited on more distal parts. This lithofacies records increasing generation and resedimentation of scoriaceous and hyaloclastic debris as the summits of the arc volcanoes grew nearer to sea level. (3) the primary volcanic lithofacies—monolithologic dacite pyroclastic flows were produced during the eruption of differentiated magmas, which climaxed the growth of the island arc. Basalt lava flows were fed from fissures that extended down the apron within the back-arc basin.

Pyroclastic rocks of the back-arc apron were blanketed with silty basinal turbidites (epiclastic facies) that record abrupt cessation of volcanism and erosion of the arc within about 10 m.y. of ophiolite generation, reflecting the temporal episodicity of back-arc basins.

It is predicted from this study that the frontal-arc side of back-arc spreading centers is preferentially preserved in the geologic record relative to the center of the basin. It is suggested that the "hot" frontal-arc side of the basin is prone to intra-plate volcanism but is unaffected by faulting subsequent to basin initiation. Several factors lead to slumps occurring more frequently on the arc flank of back-arc basins than in any other tectonic setting, except perhaps intra-arc marine basins.

INTRODUCTION

Modern back-arc basins may be distinguished from normal ocean basins petrologically or by their positions behind active or inactive trench systems (Taylor and Karner, 1983). It is unlikely for such diagnostic features to be preserved in ancient back-arc basins, which commonly undergo metamorphic and structural modifications during emplacement in orogenic zones. The nature and timing of deposition of sediment covers on top of ophiolitic sections have proven more diagnostic for determining original plate-tectonic setting (Tanner and Rex, 1979; Hopson and others, 1981, 1986; Sharp, 1980; Kimbrough, 1982, 1984). The present study supports Karig and Moore's (1975) assertion that those back-arc basins isolated from terrigenous sediment influx may show the following simple, uniform sedimentation patterns. The first is (1) lateral and vertical differentiation of facies due to progradation of a thick volcaniclastic apron into a widening marginal basin; such an apron may extend for more than 100 km from a volcanic island and grow to a thickness of 1 km in 5 m.y. (Lonsdale, 1975). This phase is followed by (2) blanketing of the apron with a thin sheet of muds, silts, and sands eroded from the arc after volcanism and spreading have ceased. This cycle reflects the temporal episodicity of back-arc basins, which appear to form in 10 m.y. or less, possibly in response to reorganization of plate motions (Taylor and Karner, 1983).

Modern back-arc basins have been penetrated in more sites by the Ocean Drilling Program (formerly the Deep Sea Drilling Project) than has any other Holocene sedimentary-tectonic domain (Klein and Lee, 1984). Yet, very few detailed field studies have been carried out on ancient, uplifted back-arc basin assemblages. Excellent exposures of the Middle Jurassic Gran Cañon Formation on the rugged desert island of Cedros (Baja California, Mexico) provide an opportunity for detailed facies analysis of a deep-marine back-arc volcaniclastic apron and its arc-ophiolite substrate.

GEOLOGIC SETTING AND PREVIOUS WORK

Kimbrough (1982, 1984), through field, petrological, and geochronological studies, recognized a Middle to Late Jurassic history of arc volcanism, rifting, and sedimentation on Cedros Island in Baja California, Mexico. Similar Middle to Upper Jurassic arc-ophiolite assemblages 800 km to the north in the Klamath Mountains, the Sierra Nevada, and the Coast Ranges of Alta California have been compared to modern fringing-arc systems of the western Pacific (Saleeby, 1983). In modern systems, rifting of a volcanic arc to initiate back-arc spreading may occur along either side of, or within, the line of volcanoes. The presence or preservation of a remnant arc (inter-arc basin of Karig, 1970, 1971a, 1971b) is thus not a necessary condition for a marginal basin to be considered a back-arc basin, according to Taylor and Karner (1983). These authors defined back-arc basins as all marginal basins (that is, small ocean basins) for which the origin is inferred to be subduction related. I am aware of no examples in the literature of a small ocean basin generated by seafloor spreading in a fore-arc region contempora-

Geological Society of America Bulletin, v. 100, p. 218–233, 8 figs., February 1988.

neous with ongoing arc magmatism. The ophiolitic rocks on Cedros Island formed in close proximity to, and contemporaneous with, island-arc volcanic and intrusive rocks (Kimbrough, 1982, 1984); thus, these basement rocks and their volcaniclastic cover represent a fragment of an arc–back-arc basin assemblage.

Basement rocks of Cedros Island are divisible into two types, arc and ophiolitic rocks. The Choyal Formation, in the north part of Cedros Island (Fig. 1), has been interpreted as a fossil volcanic-arc eruptive center (Jones and others, 1976). It is composed largely of pillow lavas of tholeiitic and calc-alkaline affinities and is intruded by small tonalite and granodiorite stocks that have yielded U-Pb zircon ages ranging from 166 to 160 Ma (Kimbrough, 1982). On the southern half of Cedros Island, a dismembered ophiolite has yielded a U-Pb zircon age of 173 Ma (Kimbrough, 1982). The oldest stock in the arc basement may thus be slightly younger than the ophiolite and overlaps in age with the back-arc apron (discussed below), although minor discordance in the zircon data (as well as analytical uncertainty) places these distinctions near the limits of detection. The arc lavas intruded by the stocks are, therefore, probably slightly older than the ophiolite (Kimbrough, 1982). These age relationships suggest that the ophiolite formed by extensional rifting of an arc that remained active after rifting (Kimbrough, 1982).

The arc volcanic rocks of the Choyal Formation and the pillow basalts of the Cedros Island ophiolite are conformably overlain by basal strata of the Gran Cañon Formation on the northwest and southeast flanks of the Pinos syncline, respectively (Fig. 1). The Gran Cañon Formation records progradation of a deep-marine volcaniclastic apron, composed largely of resedimented pyroclastic debris and lesser pyroclastic flows and lava flows (Busby-Spera and Keller, 1985).

Field and geochronological data support the interpretation that back-arc rifting was immediately followed by deposition of the Gran Cañon Formation, which accumulated within 10 m.y. of ophiolite generation (Kimbrough, 1982). Pelagic sedimentary rocks are absent below tuffs of the Gran Cañon Formation (Fig. 2), and there is evidence of hydrothermal alteration of the basal tuffs along with the ophiolitic rocks (Kimbrough, 1982, 1984). *Bositra buchim*, which is most abundant in Callovian strata of the Bedford Canyon Formation, is reported from the middle part of the formation (Jones and others, 1976); given the Decade of North American Geology time scale, this suggests an age between approximately 163 and 169 Ma. A dacite pyroclastic flow near the top of the formation has yielded a U-Pb zircon age of 164 Ma (Kimbrough, 1982).

The Coloradito Formation, which conformably overlies the Gran Cañon Formation (Fig. 1), includes slump-folded sandstones and scaly matrix argillites with exotic blocks of quartzite, Paleozoic limestone, and Triassic chert (Kilmer, 1977; Boles and Landis, 1984), as well as locally derived blocks of the Choyal and Gran Cañon Formations. It is interpreted as a slope facies that records accretion of the Middle to Upper Jurassic arc-ophiolitic assemblage against a continent or continental fragment, and the overlying Eugenia Formation represents the fill of a submarine channel that formed on this slope (Boles and Landis, 1984). The time of influx of continental detritus in the Coloradito Formation is poorly constrained because fossil and radiometric age determinations probably come from resedimented blocks; however, the Eugenia Formation, which appears to be coeval with the upper part of the Coloradito Formation, has yielded Late Jurassic fossils (Boles and Landis, 1984). Continental accretion of the Jurassic arc-rift system thus took place shortly after the rift-

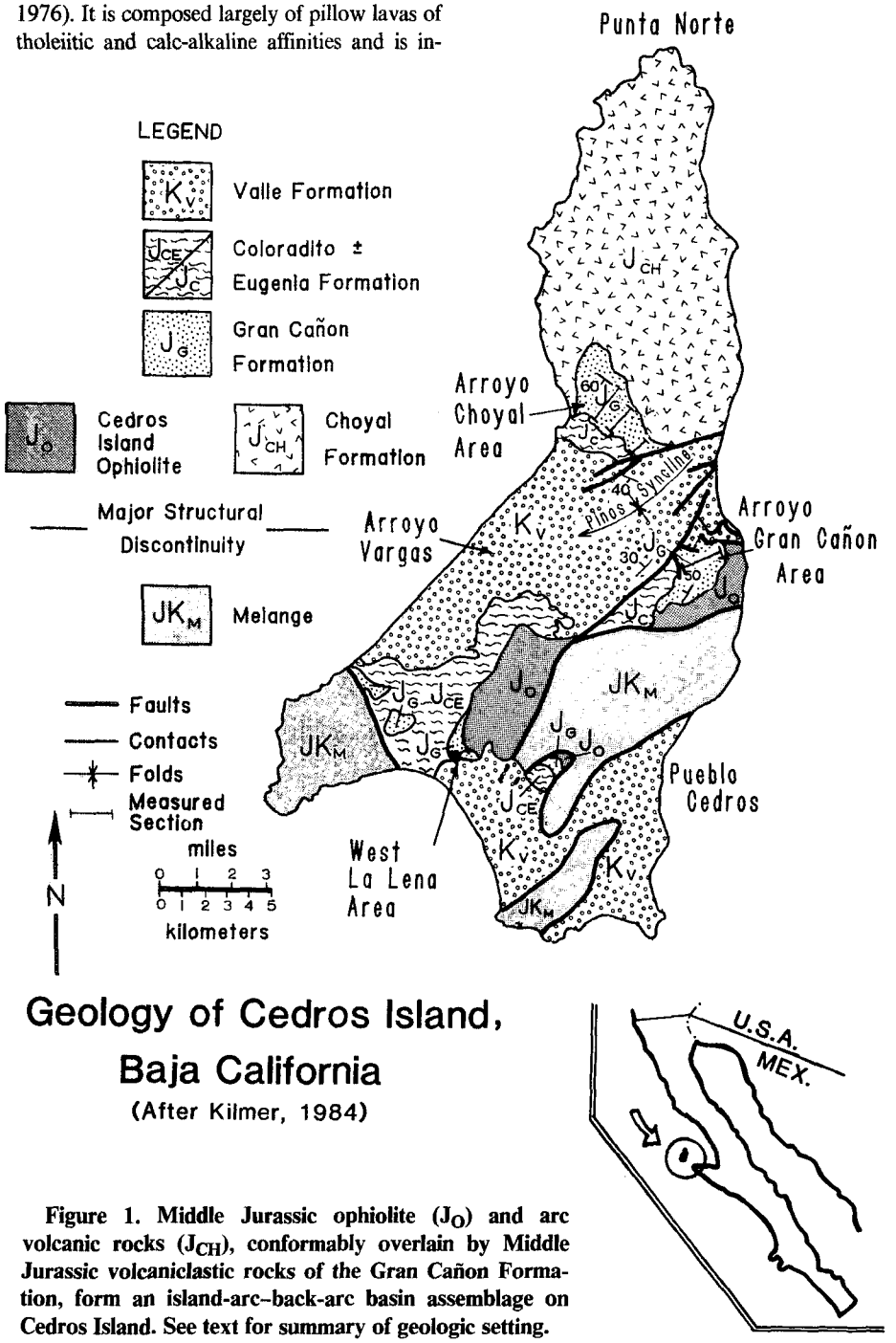

Geology of Cedros Island, Baja California
(After Kilmer, 1984)

Figure 1. Middle Jurassic ophiolite (J_O) and arc volcanic rocks (J_{CH}), conformably overlain by Middle Jurassic volcaniclastic rocks of the Gran Cañon Formation, form an island-arc–back-arc basin assemblage on Cedros Island. See text for summary of geologic setting.

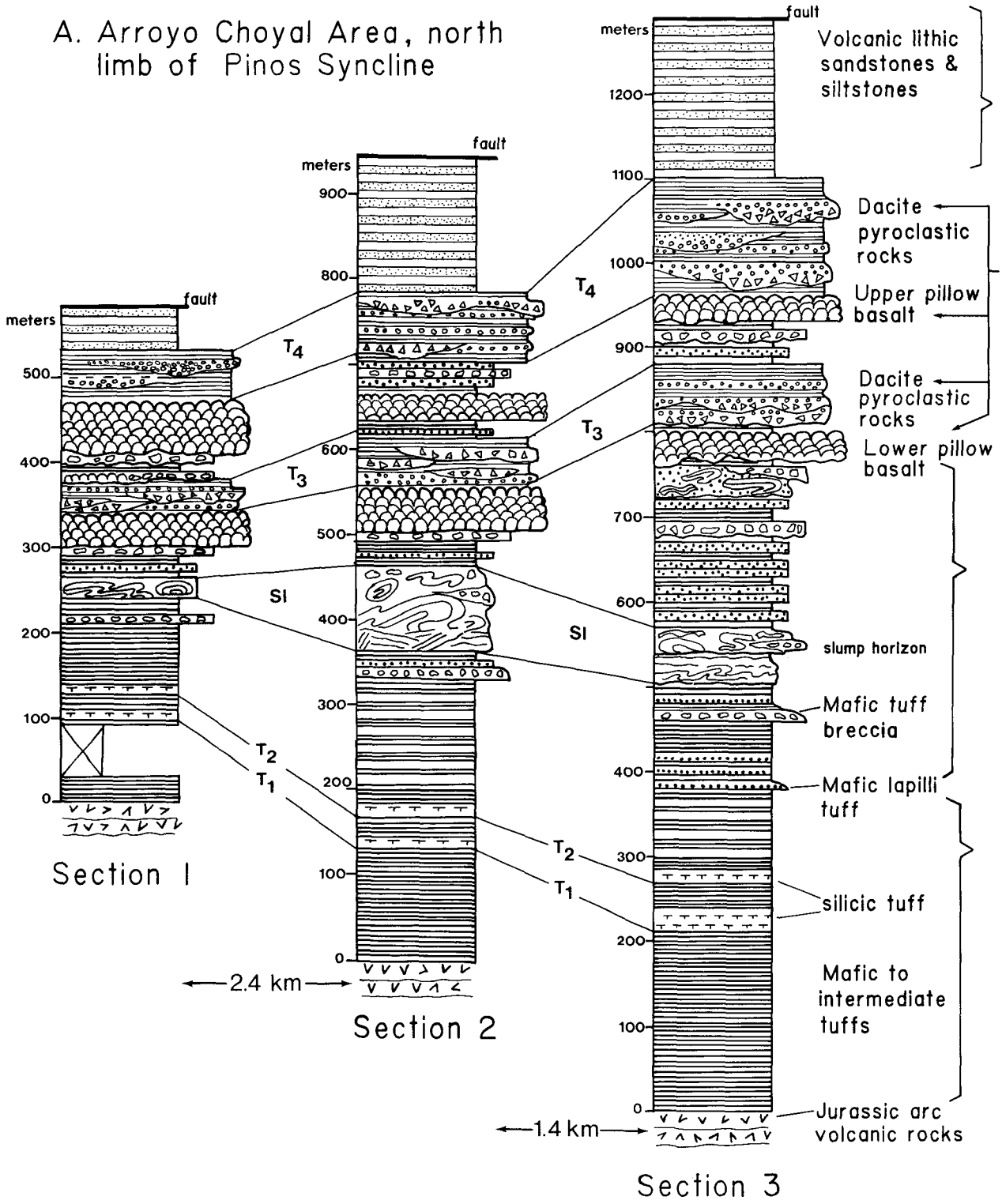

Figure 2. Measured sections of the Gran Cañon Formation, Cedros Island; localities of sections A (1, 2, 3), B, and C are plotted in Figures 1 and 3. Paleocurrent data (D) indicate a northern source for the Gran Cañon Formation, and pyroclastic debris coarsens toward the inferred northern source area (from C to B to A). Note the close correlation of lithofacies between A and B. The Arroyo Gran Cañon area is inferred to have lain approximately 15 km down-fan of the Arroyo Choyal area (A) prior to folding of the Pinos syncline. T_1 to T_4 and SI are marker horizons mapped in Figure 3.

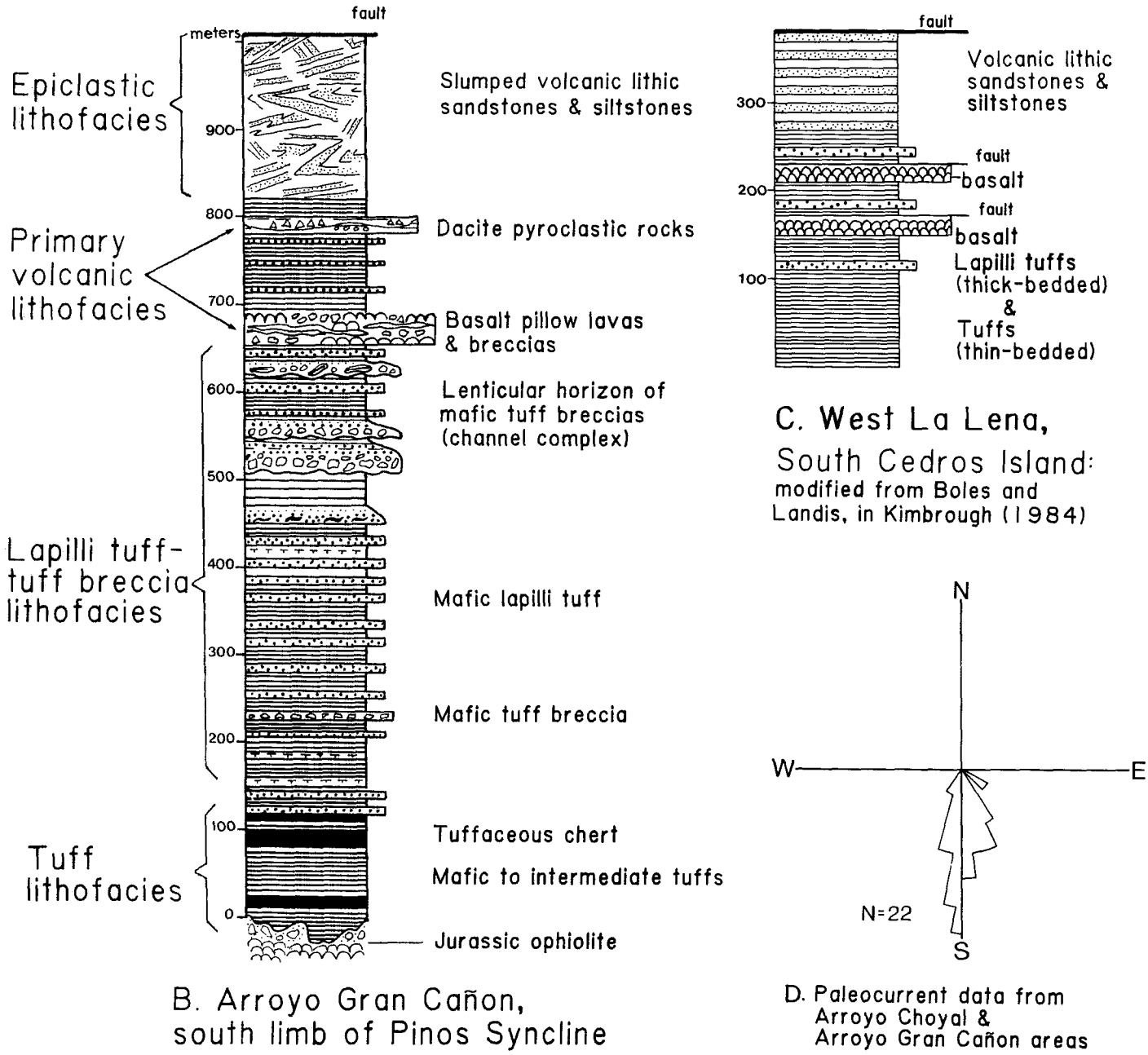

Figure 2. (*Continued*).

ing event, just as it did in Jurassic arc-rift systems of Alta California (Kimbrough, 1984; Saleeby, 1983).

Jurassic strata of Cedros Island are overlain with angular unconformity by upper Lower to Upper Cretaceous marine sedimentary rocks of the Valle Formation. These sedimentary rocks accumulated in a submarine canyon complex, structurally controlled by a deep-sea half-graben, in the fore-arc region of an arc undergoing progressive unroofing (Smith and Busby-Spera, 1987a, 1987b).

Jurassic and Cretaceous rocks of Cedros Island lie in fault contact with metamorphic rocks that have been compared to the Franciscan Complex of California by numerous workers. Serpentinite matrix mélange occurs along fault zones and yields blueschist blocks that have Cretaceous $^{40}Ar/^{39}Ar$ ages and amphibolite blocks that have mid-Jurassic $^{40}Ar/^{39}Ar$ ages; these ages probably reflect two phases of subduction in the region (Baldwin and others, 1987) and provide further evidence that the mid-Jurassic ophiolite was associated with a trench system.

STRATIGRAPHY AND STRUCTURAL GEOLOGY

The Gran Cañon Formation crops out in two major belts, along the northwest and southeast

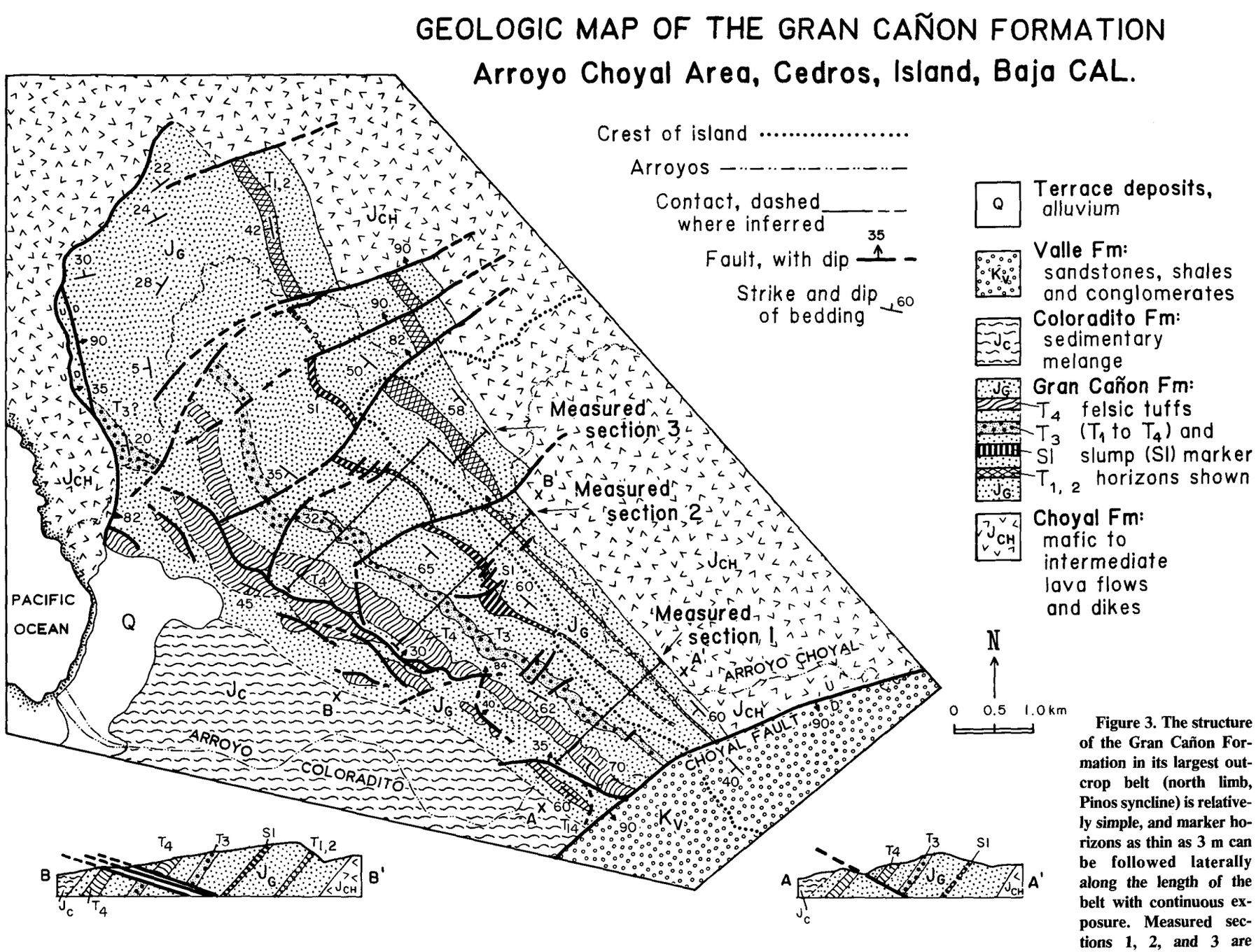

Figure 3. The structure of the Gran Cañon Formation in its largest outcrop belt (north limb, Pinos syncline) is relatively simple, and marker horizons as thin as 3 m can be followed laterally along the length of the belt with continuous exposure. Measured sections 1, 2, and 3 are shown in Figure 2.

limbs of the Pinos syncline (Arroyo Choyal and Arroyo Gran Cañon), and in a third small belt at the south end of Cedros Island (West La Lena area; Fig. 1). Several lines of evidence suggest that these three belts can be closely correlated and that they represent a volcaniclastic apron with a northern source region.

Measured sections from the two major outcrop belts (Figs. 2A and 2B) show a very similar vertical succession: a basal tuff section (herein called the "tuff lithofacies") passes gradationally upward into interbedded tuffs, lapilli tuffs, and tuff breccias (lapilli tuff–tuff lithofacies), and basalt lava flows and dacite pyroclastic rocks occur in the upper part of the formation (primary volcanic lithofacies). A measured section at the south end of the island (Fig. 2C) shows that the Gran Cañon Formation is relatively thin there and has no coarse pyroclastic debris, but at least one (or possibly two, if the section is not repeated by faults) basalt lava-flow horizon is present there. Thin-bedded volcanic lithic sandstones and siltstones (herein called the "epiclastic facies") form the uppermost part of the Gran Cañon Formation in all three outcrop belts (Figs. 2A, 2B, 2C).

A northern source for the Gran Cañon Formation is indicated by paleocurrent and other sedimentological data from the volcaniclastic rocks and lava flows. Cross-laminations in coarse-grained tuffs, lapilli tuffs, and volcanic lithic sandstones deposited from turbidites are not very common (n = 22) but show consistent southward paleocurrent directions (Fig. 2D). Additionally, elongation of pillows and lava tubes and the mapped distribution of flow-foot rubble relative to pillow lavas indicate a regional slope toward the south (Busby-Spera, in press). Basalt horizons thicken toward the inferred northern source area (from C to B to A, Fig. 2), although their widespread distribution, along with other features, suggests that they were fed by fissures that extended through the back-arc apron (Busby-Spera, in press). The abundance and grain size of mafic tuff breccias, as well as dacitic pyroclastic rocks, increases from south to north (Figs. 2A, 2B, 2C) relative to tuffs and lapilli tuffs. These paleocurrent and sedimentological data agree fairly well with north-northeast–south-southwest to northeast-southwest paleoslope orientations inferred by Kimbrough (1984) from slumped strata at the top of the Gran Cañon Formation (Fig. 2B). Furthermore, sedimentological features of the overlying Coloradito and Eugenia Formations (including elongation of clasts in olistostromes and orientation of conglomerate-filled channels; Boles and Landis, 1984) suggest that an approximately southerly regional paleoslope persisted through continental accretion of the arc–back-arc assemblage.

Prior to this study, the largest outcrop belt of the Gran Cañon Formation, the Arroyo Choyal area on the north limb of the Pinos syncline (Fig. 1), had been mapped only from aerial photographs, although the other outcrop belts were mapped in the field (Kilmer, 1984). Although access to the northern outcrop belt is extremely difficult, the exposures there are well worth the effort; marker horizons can be followed laterally for 8–9 km (Fig. 3), with continuous exposure (Fig. 4A), and the belt is traversed by 16 arroyos with water-polished outcrops.

The structure of the Gran Cañon Formation in the Arroyo Choyal area is relatively simple (Fig. 3). The strata form a homocline that dips 60° to 70° toward the south-southwest along most of its length, although dips flatten to 20° to 30° at the northwest end. One set of faults strikes perpendicular to bedding and is commonly subvertical. A younger set of faults strikes subparallel to bedding and dips 30° to 40° northeast, perpendicular to the dip of bedding (see cross sections, Fig. 3). The younger set of faults affects only the top of the Gran Cañon Formation, repeating the uppermost felsic tuff (T_4) and overlying volcanic lithic sandstones and siltstones; this set may also affect the overlying Coloradito Formation, but marker horizons are absent from this olistostromal unit. Numerous small unmapped faults cut the northwestern end of the belt of Gran Cañon Formation, where underlying basement rocks are faulted against the Gran Cañon Formation along major steeply dipping and shallowly dipping faults (Fig. 3). The Choyal fault, which bounds the belt on the southeast side, has a net vertical displacement of approximately 800 m that probably occurred during synclinal folding of the Valle Formation and subjacent strata (Kilmer, 1984).

The Gran Cañon Formation on the south limb of the Pinos syncline forms a northwest-dipping homocline cut by several subvertical faults with tens of metres of vertical displacement (Fig. 1). There is only one arroyo that traverses this outcrop belt (Arroyo Gran Cañon), and the section in Figure 2B was measured there. The localities of the three measured sections of the Arroyo Choyal area (Fig. 2A) are plotted in Figure 3.

SEDIMENTOLOGY

Sedimentary structures and textures of marine pyroclastic rocks can be used to infer volcanic and hydrodynamic processes of subaqueous deposition and to construct facies models for marine pyroclastic accumulations within or adjacent to volcanic arcs (Busby-Spera, 1986; C. J. Busby-Spera and J.D.L. White, unpub. data; White and Busby-Spera, in press). Detailed facies analysis of subaerially deposited pyroclastic rocks has been carried out in many modern arc settings, but relatively few facies models exist for marine pyroclastic rocks, which nonetheless represent a significant fraction of the geologic record (Fisher and Schmincke, 1984).

The terminology for volcaniclastic rocks used herein follows that summarized by Fisher and Schmincke (1984). Pyroclastic rocks are composed of fragments that originate from volcanic eruptions or as a direct consequence of an eruption (including unconsolidated pyroclastic debris remobilized by wind or water). Pyroclastic rocks are recognized by the presence of pumice shreds, glass shards, angular volcanic lithic fragments, euhedral crystals, or other delicate fragments. Epiclastic volcanic fragments are derived from weathering and erosion of volcanic rocks and thus may, but commonly do not, record penecontemporaneous volcanism. Mixed pyroclastic-epiclastic rocks, defined as having 25%–75% pyroclasts, are referred to as "tuffaceous sandstones," "tuffaceous siltstones," and so on. The standard granulometric classifications of pyroclasts (blocks $\geq$64 mm, lapilli 2–64 mm, and ash $\leq$ 2 mm) and their end-member or mixture rock descriptions (for example, tuff is $\geq$75% ash-sized particles; lapilli tuff has $\geq$25% lapilli, $\geq$25% ash, and $\leq$25% blocks; tuff breccia has $\geq$25% blocks and $\geq$25% ash $\pm$ lapilli) are used herein.

The Gran Cañon Formation is herein divided into three lithofacies that record the progradation of a volcaniclastic apron into a back-arc basin. These include (in ascending order, Fig. 2) the tuff lithofacies and the lapilli tuff–tuff breccia lithofacies, both representing pyroclastic material that was resedimented to varying degrees, and the primary volcanic lithofacies, which includes dacite pyroclastic rocks and basalt flows. A fourth lithofacies, the epiclastic lithofacies, caps the Gran Cañon Formation and consists of volcanic lithic sandstones and siltstones that record erosion of the arc after volcanism ceased.

Tuff Lithofacies

Mafic to intermediate thin-bedded vitric tuffs and crystal-vitric tuffs compose the lower part of the Gran Cañon Formation but occur throughout it, except in the epiclastic lithofacies at the top of the formation (Fig. 2). Horizons of thin-bedded silicic vitric tuff and crystal-vitric tuff also occur in the tuff lithofacies. Mafic to intermediate tuffs are green to brown in color, and silicic tuffs are buff to white (Fig. 4B). All of the tuffs are zeolitized, but relict shards are visible in thin sections of medium- to coarse-grained samples. Small euhedral crystals of plagioclase and clinopyroxene occur in the mafic to intermediate tuffs, whereas plagioclase and quartz $\pm$ hornblende occur in the silicic tuffs. Some of the mafic to intermediate tuffs that have a less waxy,

Figure 4A. Oblique aerial photograph of Jurassic rocks on the north limb of the Pinos syncline, Arroyo Choyal area (viewed toward the northeast); high ridge in background is lava flows and intrusions of the Choyal Formation, marker horizons ($T_{1\&2}$, T_3, T_4) of the overlying Gran Cañon Formation dip toward viewer, and the valley in the foreground (Arroyo Coloradito) is underlain by the Coloradito Formation. (The low, sharp ridge in lower right is the Cretaceous Valle Formation.)

Figure 4B. Dark-colored intermediate to mafic tuffs and light-colored silicic tuff (map unit T_2), basal Gran Cañon Formation, Arroyo Choyal area.

more granular appearance probably have an epiclastic component (silty tuffs, tuffaceous siltstones), but the presence of cherts in the basal Gran Cañon Formation (Fig. 2B) indicates that pelagic-hemipelagic rain of terrigenous sediment was minimal.

The thin-bedded tuffs of the Gran Cañon Formation are laminated and very well sorted. Beds or laminae of very fine-grained to fine-grained, rare medium-grained, and very rare coarse-grained tuff occur in random vertical succession in the tuff lithofacies, even within single tuff layers of uniform composition. Scour-and-fill structures and graded beds are absent in the thin-bedded tuffs.

The geometry and distribution of individual tuff layers, as well as sections of tuff as a whole, were mapped and measured with the goal of understanding their origin. This type of analysis could be carried out only in the basal 100–380 m of the Gran Cañon Formation (labeled "tuff lithofacies" in Fig. 2) because the original geometry of tuff layers higher in the section is commonly obscured by slumping or by scour-and-fill structures at the base of interstratified coarse-grained deposits. Mappable tuff layers in the tuff lithofacies section, including two silicic tuff layers in the predominantly intermediate to mafic tuff lithofacies (see T_1 and T_2, Fig. 3), show lateral continuity along the 9.5 km length of the northern outcrop belt. The mapped silicic tuff layers double in thickness over the 3.8 km between measured sections (T_1 from 3 to 6 m, and T_2 from 11 to 24 m, Fig. 2A) and continue to thicken toward the northwest end of the outcrop belt as shown in Figure 3. The tuff lithofacies at the base of the Gran Cañon Formation as a whole also doubles in thickness along the length of the northern outcrop belt (Fig. 2A). This section is much thinner on the south limb of the Pinos syncline than it is on the north limb (Fig. 2B), and the presence of cherts on the south limb indicates that ash did not reach the distal part of the back-arc apron as frequently as it did the proximal part. Silicic tuff layers in the Gran Cañon Formation are unusually thick relative to subaerial or submarine ash layers reported in the literature, which are measured in centimetres rather than metres (Thorarinsson, 1954; Ninkovich and others, 1964; Williams and Goles, 1968; Horn and others, 1969; Bowles and others, 1973; Jezek, 1976; Ninkovich and others, 1978; Watkins and others, 1978; Carey and Sigurdsson, 1980).

Deep-sea ashes may be emplaced by the following mechanisms: (1) *deep-marine eruptions*, which should result in inefficient dispersal of ash (Karig, 1983; Busby-Spera, 1986), although no isopach maps are yet available for such deposits; (2) *submarine fallout from subaerial to shallow-marine eruptions*, which results in an ash layer of great areal extent that wedges very gradually away from the source over distances of hundreds of kilometres (Watkins and others, 1978; Carey and Sigurdsson, 1980); or (3) *remobilization of ash* following a subaerial or shallow-marine eruption. In this case, ash may be washed from the flanks of an island volcano and/or resuspended in shallow-marine environments by storm waves and currents and carried to deep-marine environments, in a manner analogous to

turbid flows of clay and silt along modern continental margins. In an arc flank or back-arc setting, where broad shelves do not intervene between basinal and subaerial environments to act as a trap for coarse sediment, the deposits of turbid flows generated by remobilization of ash will be intimately interstratified with coarser resedimented pyroclastic debris (White and Busby-Spera, in press). The third mechanism, therefore, cannot be called on to explain the very thick section of tuffs at the base of the Gran Cañon Formation, although it is viable for tuffs interstratified with coarse debris in the middle and upper parts of the section (Fig. 2). This coarse debris is interpreted (below) to be the product of shallow-marine to subaerial phreatomagmatic and pyroclastic eruptions that undoubtedly produced ash layers as well; however, the geometry of tuffs in the basal third of the Gran Cañon Formation precludes this mode of origin.

It is inferred herein that the tuff lithofacies at the base of the Gran Cañon Formation (Fig. 2) resulted from deep-marine eruptions during the early stages of arc evolution and that these eruptions supplied dilute sediment gravity flows of ash to the back-arc basin. The unusually great thickness and rapid lateral variation in thickness of individual tuff layers in the Gran Cañon Formation are similar to those in proximal subaerial fallout layers, which may be metres thick and show rapid lateral thickness variation (as much as 10× within 20 km of the vent); however, proximal subaerial fallout tephras are much coarser in grain size (with abundant lapilli-sized fragments) than are tuff layers of the Gran Cañon Formation. This may indicate that dispersal of larger fragments is hampered by suppression of the eruption column by hydrostatic pressure in a deep-marine environment, leading to very efficient proximal-to-distal sorting of the tephra. Alternatively, large pyroclasts may never have been generated in abundance if extreme phreatomagmatic fragmentation occurred; however, the geometry and grain size of mappable silicic tuff layers in the tuff lithofacies at the base of the Gran Cañon Formation preclude their origin as such "phreatoplinian" deposits. Phreatoplinian deposits are as widely dispersed as plinian airfall, with the coarsest particles (pumice) dispersed over an area comparable to that in plinian eruptions (Self and Sparks, 1978; Walker, 1981).

The very good sorting and stratification in the tuff lithofacies section are typical of subaqueous fallout tuffs (that is, ashes that have settled through water; Fisher, 1964), but the geometry and distribution of individual tuff layers and the tuff lithofacies section as a whole suggest that they were deposited from sediment gravity flows (albeit extremely dilute ones incapable of scouring their substrate). The fact that the cross-paleocurrent thickness of the tuff lithofacies section as a whole doubles along with the thickness of mappable tuff layers (Fig. 2A) suggests that turbid flows followed a paleo-low in the back-arc substrate. A greater thickness of somewhat coarser pyroclastic debris accumulated in this paleo-low throughout the evolution of the back-arc apron (compare columns 3 and 1, Fig. 2A). Lateral thickness variation in the tuff lithofacies section thus reflects the topography of the basin floor rather than primary fallout distribution. The tuff lithofacies is much thinner on the south limb of the Pinos syncline than it is on the north limb (Fig. 2). This down–paleo-current thinning supports the interpretation that turbid flows, which have lower areal distribution than does subaqueous fallout from subaerial or shallow submarine eruptions, played an important role in the accumulation of the basal tuff section. Fewer turbid flows arrived at more distal parts of the apron, allowing cherts to form there (Fig. 2B). These turbid flows were probably generated directly by deep-marine eruptions.

Lapilli Tuff–Tuff Breccia Lithofacies

Medium- to thick-bedded, fine- to coarse-grained lapilli tuffs and very thick-bedded tuff breccias are interstratified with thin-bedded tuffs in the middle part of the Gran Cañon Formation. The fine-grained lapilli tuffs are green in color and are composed of an unsorted, zeolitized mixture of mafic ash (plagioclase+clinopyroxene+block-shaped shards) and small mafic lapilli (unvesiculated to scoriaceous). This material forms the matrix for the tuff breccias and the coarse-grained lapilli tuffs, which bear angular to subrounded fragments of basalt, andesite, and minor dacite. Rare micrite blocks with molluscs and clams occur in tuff breccias both in the Arroyo Choyal area (Kimbrough, 1982) and in the Arroyo Gran Cañon area (this study) but have not yielded age-diagnostic fossils.

Fine-grained lapilli tuffs of the lapilli tuff–tuff breccia lithofacies are massive to very indistinctly stratified and nongraded and have nonerosive bases, whereas the coarse-grained lapilli tuffs show weak grading of larger clasts and minor scouring of underlying tuffs. Tuff breccias occur throughout the lapilli tuff–tuff breccia lithofacies on the north limb of the Pinos syncline and increase in abundance upsection (Fig. 2A). Tuff breccias are less common on the south limb of the Pinos syncline and are largely restricted to a complex of channels at the top of the lapilli tuff–tuff breccia lithofacies (Fig. 2B). This channel complex is centered over Arroyo Gran Cañon and does not extend laterally for more than a kilometre from the section measured there (Fig. 2B).

Tuff breccias on the north flank of the Pinos syncline (Fig. 5A) occur as (1) nonchannelized, nongraded, unsorted deposits lacking clast alignment or stratification (Fig. 6A), with nonerosive bases and steep depositional margins draped by overlying strata, or, less commonly, (2) flat-based to erosively based, nonchannelized, nongraded to incompletely graded, nonstratified tuff breccia gradationally to sharply overlain by nonstratified lapilli tuff. Tuff breccias on the south flank of the Pinos syncline (Fig. 5B) occur as channelized, erosively based, well-graded deposits that have flat clast alignment and abundant intraclasts; these grade upward into lapilli tuffs and tuffs that are commonly stratified (Fig. 6B). Each tuff breccia scoured and filled its own channel; individual channels, although 10 m or more deep (Fig. 5B), are commonly less than 100 m wide (measured across paleo-slope inferred from paleo-current data).

Slump deposits are common throughout the lapilli tuff–tuff breccia lithofacies (Fig. 2). These slumped horizons are much thicker (as much as 100 m), much more laterally extensive (as much as 7 km, Fig. 3), and much more common on the north limb of the Pinos syncline than on the south limb, where they are each less than a few metres thick and continue laterally only tens of metres. Slumped horizons of the lapilli tuff–tuff breccia lithofacies consist of recumbently folded or chaotically contorted bedded intervals, bounded above and below by undisturbed strata. Folded fine-grained tuff intraclasts as much as tens of metres long are common as blocks or slabs in tuff breccias throughout each slump horizon, indicating that slumping occurred at the surface of the apron (Fig. 6C). Intervals within some slumped horizons that had abundant cohesive ash layers locally broke into blocks and slabs ("broken formation") rather than folding. In the thickest slump horizon, mapped as a marker horizon for a distance of 8 km (Fig. 3), undisturbed remnants of the original stratigraphy are preserved only at one locality for a distance of 300 m. This slump horizon locally has very large blocks of fossiliferous micrite.

The polylithologic nature of large fragments (blocks to coarse lapilli) in beds of the lapilli tuff–tuff breccia lithofacies indicates mixing of volcanic debris, probably by downslope remobilization of unstable deposits. The compositionally uniform mafic lapilli-tuff matrix of these strata, however, suggests that the unstable ac-

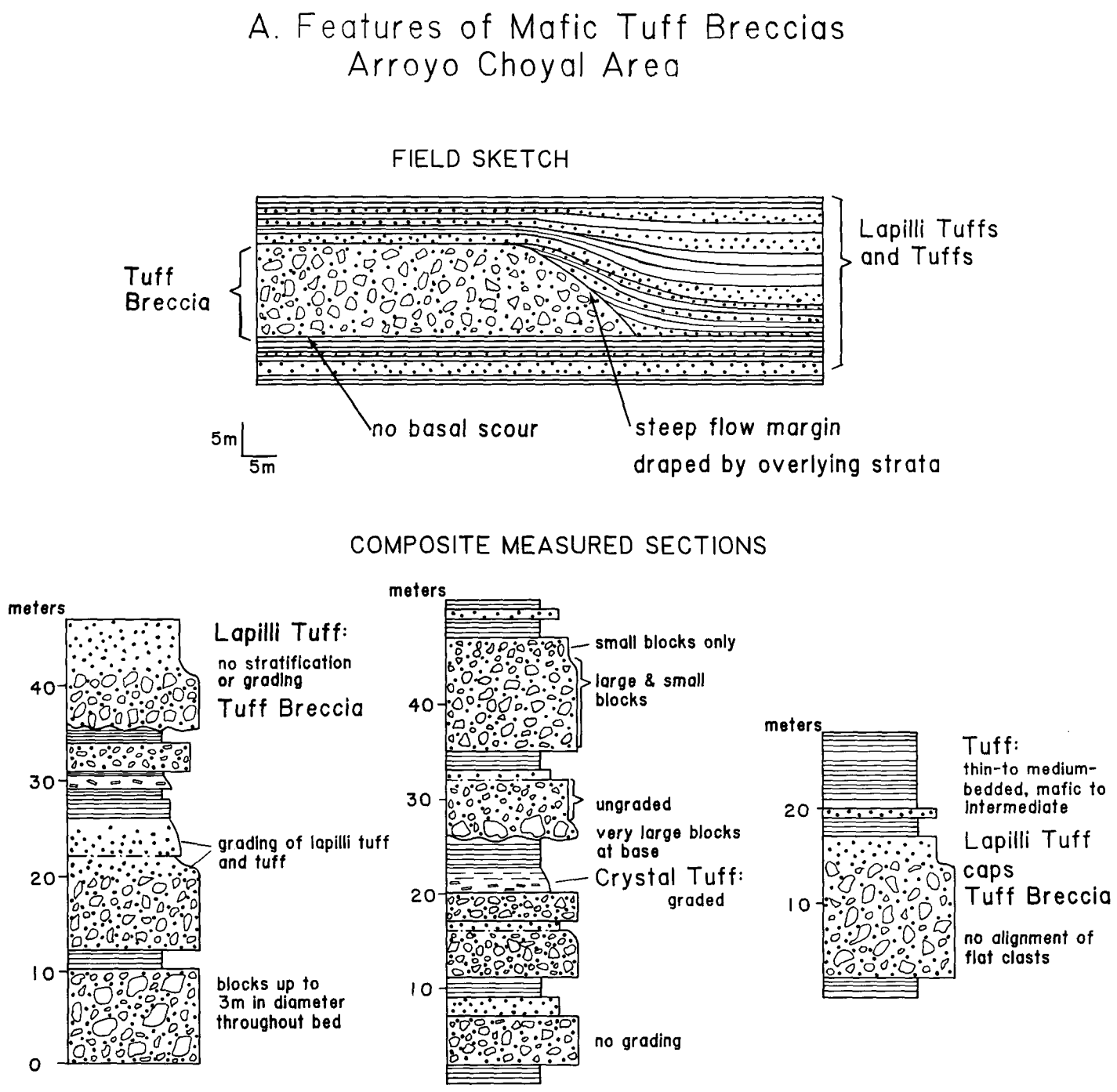

Figure 5. Depositional features of mafic tuff breccias of the Gran Cañon Formation (lapilli tuff–tuff breccia lithofacies). A. In relatively proximal regions of the back-arc apron (Arroyo Choyal area), tuff breccias occur either as nonchannelized, nongraded bodies that have steep depositional margins or, less commonly, as flat to erosively based, nonchannelized, nongraded to incompletely graded tuff breccias capped by nonstratified lapilli tuff. B. In relatively distal regions of the of the back-arc apron (Arroyo Gran Cañon area), tuff breccias are strongly channelized and erosively based, show abundant intraclasts and pronounced vertical grading, and pass upward into graded, stratified lapilli tuffs and tuffs.

cumulations were the direct result of explosive volcanic eruptions. The blocky (rather than bubble-wall) shape of the shards indicates fragmentation by steam explosions to form hyaloclastites. The rare shelly micrite blocks, resedimented from shallow water, suggest that at least part of the volcanic edifice lay close to sea level. The outsized shelly micrite blocks in the largest slump horizon (Sl, Figs. 2 and 3) provide evidence that slumping on the surface of the back-arc apron was triggered by seismic events at this edifice.

Sedimentological features of the tuff breccias indicate that debris flows and density-modified grain flows (terminology of Lowe, 1982) were deposited across the width of the back-arc apron in relatively proximal areas, represented by the Arroyo Choyal area. On relatively distal parts of

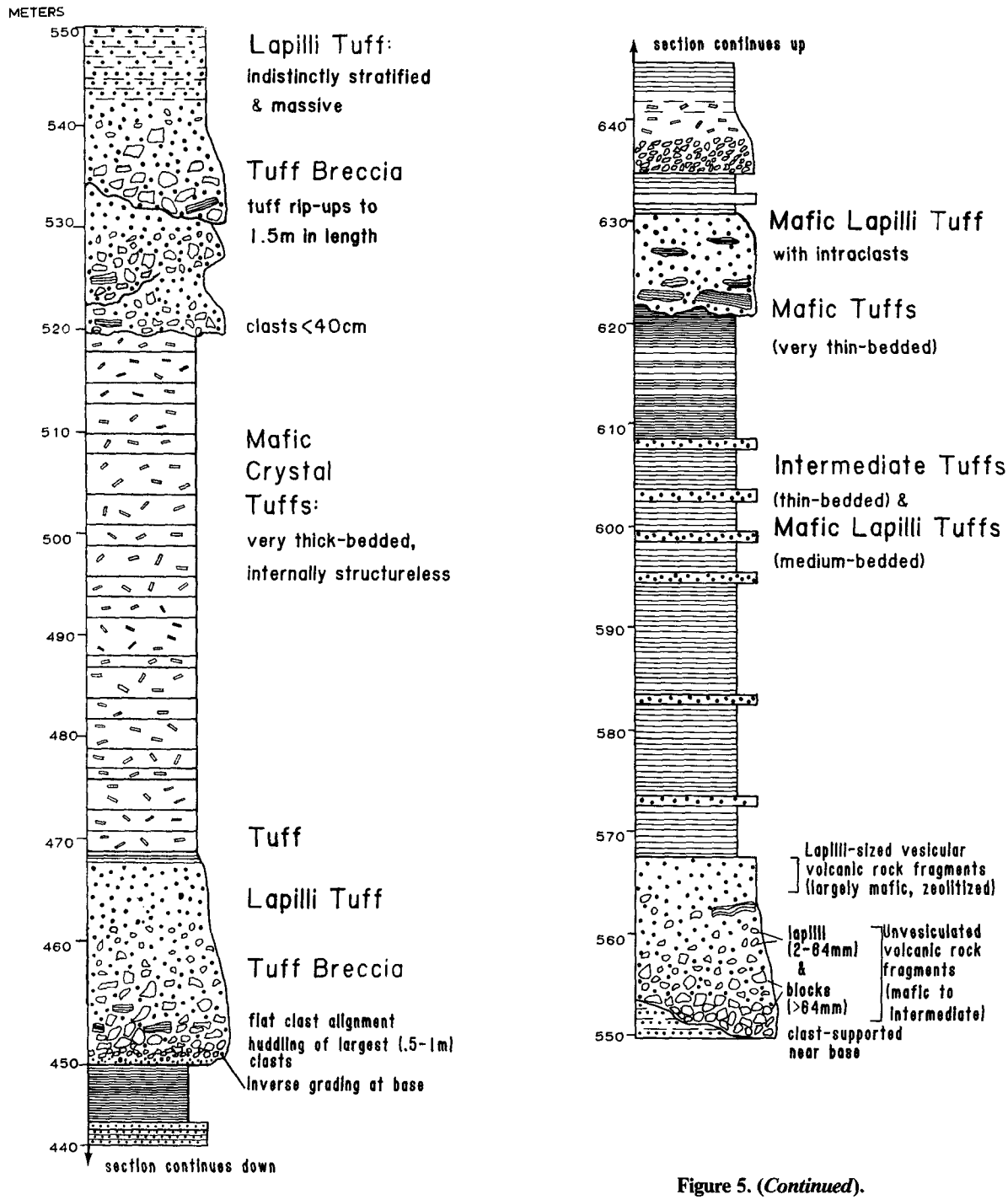

Figure 5. (*Continued*).

the apron (Arroyo Gran Cañon area), high-density turbidites scoured channels in complexes that aggraded vertically but were confined to narrow regions, perhaps by topographic lows on the apron's surface or in its substrate. The greater development of slumped horizons on relatively proximal parts of the back-arc apron, compared to relatively distal parts, may have resulted from higher surface slopes due to rapid buildup of coarse-grained debris, analogous to modern alluvial fans. Debris flows were able to come to rest on more proximal parts of the apron, whereas more turbulent flows continued down the apron to be deposited in more distal areas. Additionally, some turbulent flows may have evolved from debris flows by incorporation of water during down-apron transport ("flow transformations" of Fisher, 1984).

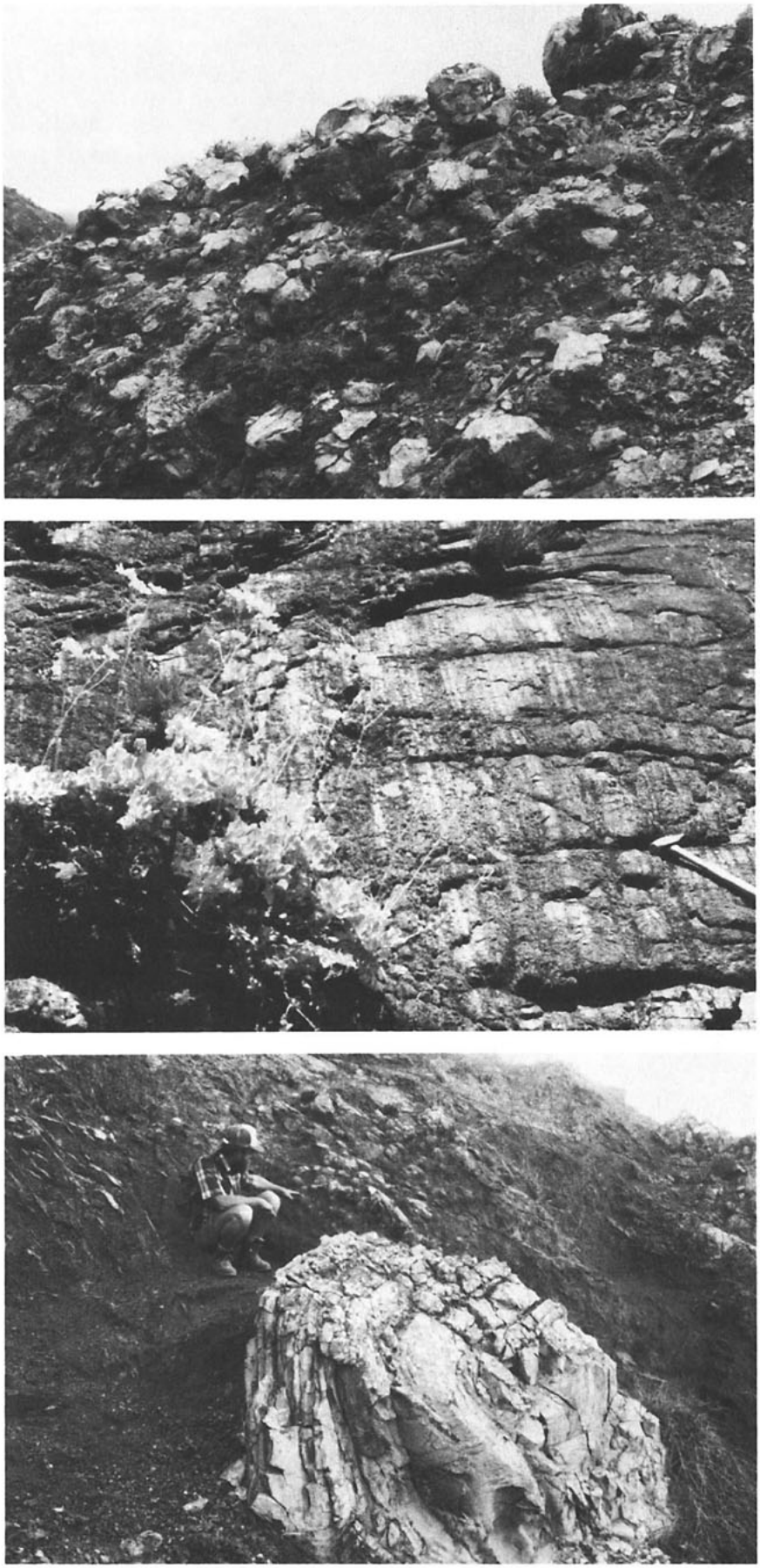

Figure 6. Lapilli tuff–tuff breccia lithofacies. A. Massive, unsorted tuff breccias of the Arroyo Choyal area (Fig. 5A) represent debris flows deposited on relatively proximal parts of the back-arc apron. B. Stratified lapilli tuffs and tuffs; these lie in the upper part of a graded bed that has a basal interval of clast-supported tuff breccia (not shown). The total thickness of each graded bed commonly exceeds 10 m (Fig. 5B), representing high-density turbidites deposited in channel complexes on relatively distal parts of the back-arc apron (Arroyo Gran Cañon area). C. Folded tuff intraclasts in tuff breccias within slump-folded horizons indicate instability on the surface of the back-arc apron, particularly in proximal areas (Fig. 5A).

Primary Volcanic Lithofacies

The primary volcanic lithofacies of the Gran Cañon Formation includes (Figs. 2A, 2B) (1) dacite pyroclastic rocks, primarily monolithologic dacite tuffs, lapilli tuffs, and tuff breccias, in sequences as much as 80 m thick, and (2) basalt lava flows, pillow lavas, pillow breccias, lava tubes, and massive flows, in horizons as much as 70 m thick. Monolithologic volcaniclastic and volcanic rocks of the primary volcanic lithofacies represent material transported directly from vent regions to the site of deposition, with minimal resedimentation. Polylithologic tuff breccias, lapilli tuffs, and tuffs of the lapilli tuff–tuff breccia lithofacies (described above) are interstratified with dacites and basalts of the primary volcanic lithofacies (Fig. 2).

Basalt lava flows of the Gran Cañon Formation bear phenocrysts of clinopyroxene and plagioclase; whole-rock chemistry and microprobe analyses indicate that they are weakly alkaline tholeiites (Kimbrough, 1982). Kimbrough (1982) proposed that the pillow lavas form a laterally persistent horizon in the Arroyo Choyal and Arroyo Gran Cañon sections in the Pinos syncline and sections in the southern part of the island (see Figs. 3A, 3B, 3C).

The structure and organization of basalt lava flows of the Gran Cañon Formation are described in detail elsewhere (Busby-Spera, in press). A great deal of information on the morphology of modern sea-floor lavas has been applied to the interpretation of ancient lavas, but the detailed three-dimensional observations possible in on-land studies have also contributed much to our understanding of processes (Carlisle, 1963;

Dimroth and others, 1978; Moore and Charlton, 1984; Staudigel and Schmincke, 1984; Yamagishi, 1985). Basalt lava flows of the Gran Cañon Formation show a great contrast in structure and organization between proximal and distal positions on the back-arc apron (Busby-Spera, in press). In proximal positions, the lava flows are pillowed throughout, and pillows are large and unbroken, whereas lava flows in distal positions are thinner and are dominated by flow-foot rubble and small pillows. Quite significantly, other features in distal areas indicate close proximity to a vent; these features include large, whole lava tubes and stacked, collapsed lava tubes, as well as minor massive to megapillowed lava. The intimate interstratification of proximal and distal basalt facies on a relatively distal part of the back-arc apron, as well as the widespread nature of the basalt lava flows relative to coarse-grained pyroclastic debris (Fig. 2), is the result of a fissure that is inferred to have extended down the back-arc apron (Busby-Spera, in press).

Dacite pyroclastic rocks of the Gran Cañon Formation are light buff in color and bear fresh crystals of zoned plagioclase and green hornblende, ±quartz, in a fine-grained zeolitized matrix with relic bubble-wall shards. Lapilli tuffs and tuff breccias bear nonvesicular to poorly vesiculated dacite (juvenile) lithic fragments or highly vesiculated juvenile fragments (pumice) or both (Fig. 7). Accidental fragments of andesite and basalt occur but are not abundant. Dacite lithic fragments commonly show copper mineralization.

Sedimentological features of dacite pyroclastic rocks in the Gran Cañon Formation support the interpretation of a northern source area for the volcaniclastic apron. The thickness and overall grain size of dacite pyroclastic deposits decrease markedly between the north and south limbs of the Pinos syncline (Figs. 7A and 7B), and there are no dacite pyroclastic rocks at the south end of Cedros Island (Fig. 2C). In both proximal and distal areas, dacite tuff breccias and lapilli tuffs commonly form graded beds, 2 to 18 m thick, deposited by a turbidity-current mechanism; however, pumice lapilli and blocks are much more common in distal areas than in proximal areas (Fig. 7). This indicates that pumiceous flows had greater mobility, due to lower densities, than did lithic-rich flows. The pumiceous flows may have resulted directly from eruptions of highly vesiculated debris that entirely bypassed proximal parts of the apron. Alternatively, some pumiceous flows may have become segregated from a denser underflow of lithic-rich debris and may have traveled farther down the apron as an independent flow. For example, the pumiceous graded bed with small block-sized to lapilli-sized lithic fragments at its base (middle column, Fig. 7B) may be the distal equivalent of a coarse-grained lithic tuff breccia, such as those shown in Figure 7A. This bed, in turn, may have passed down-apron into a pumiceous bed lacking lithic fragments, similar to the beds below it as shown in Figure 7B.

Epiclastic Lithofacies

Thin-bedded sandstones and siltstones in the uppermost part of the Gran Cañon Formation were first recognized by Kimbrough (1982, 1984), who proposed that they were, at least in part, epiclastic. Petrographic and field studies by this author show that a very abrupt change, from predominantly pyroclastic to entirely epiclastic sedimentation, is recorded near the top of the Gran Cañon Formation (Fig. 2), although this stratigraphic relationship is locally obscured by faults. The absence of tuffs or tuffaceous sediments in the epiclastic section indicates that there were no longer any active subaerial volcanoes along a major segment of the arc. Fine-grained sediment was shed onto the back-arc apron by erosion of the adjacent volcano or arc segment.

Sandstones of the epiclastic lithofacies are generally thin-bedded and fine-grained silty sandstones, although minor medium-grained sandstone beds of medium thickness occur in the north limb of the Pinos syncline (closest to the inferred arc position). The silty sandstones are composed largely of a mixture of intermediate to mafic, and minor felsic, volcanic rock fragments; subordinate crystals (of plagioclase, pyroxene, hornblende, and quartz) also reflect thorough mixing of various parent volcanic materials. Pumice and glass shards are absent. Siltstones of the epiclastic lithofacies lack the waxy luster of the tuff lithofacies and are less resistant to erosion.

Sandstones and siltstones of the epiclastic lithofacies form monotonous sections that show no vertical trends in bed thickness. Sedimentary structures are generally not visible, although some beds show grading or Bouma intervals t_{cde} or t_{de}. These turbidites closely resemble the silty basinal turbidites of modern back-arc basins of the western Pacific (Klein, 1985).

Detailed mapping on the north flank of the Pinos syncline (Fig. 3) has shown that a set of faults that strikes subparallel to bedding near the top of the Gran Cañon Formation has, several times, repeated the contact between the epiclastic lithofacies and the underlying primary volcanic lithofacies (including dacite pyroclastic rocks of map unit T_4 and the underlying upper pillow basalt, Fig. 2A) in several places. Excellent exposure and lateral continuity of marker horizons in the primary volcanic lithofacies make it possible to demonstrate that these repetitions are structural, not stratigraphic. Any fault repetitions of the monotonous epiclastic section that do not bring volcanic strata to the surface would be difficult to detect; thus, the true thickness of the epiclastic section shown in Figure 2A cannot be determined with confidence. In Arroyo Gran Cañon (Fig. 2B), disruption of the epiclastic lithofacies is interpreted to have occurred in a single, large slump horizon that formed after deposition of the overlying Coloradito Formation began (Kimbrough, 1982, 1984); thus, its original thickness is not known. On the south end of Cedros Island, the top of the Gran Cañon Formation is faulted against the Valle Formation (Boles and Landis, in Kimbrough, 1982), but a similar thickness of Gran Cañon Formation is conformably overlain by the Coloradito Formation 4 km to the east (Kimbrough, 1982).

In summary, although the thickness of the epiclastic section can only be estimated at most localities, the epiclastics formed a homogeneous blanket of turbiditic silty sandstones and siltstones that covered the entire back-arc apron, with very little proximal to distal variation. The absence of submarine-fan turbidites and the presence of silty basinal turbidites in modern back-arc basins has been correlated with minimal rates of tectonic uplift in the adjacent island arc (probably <400 m/m.y.; Klein, 1985).

EVOLUTION OF ARC–BACK-ARC SYSTEMS: A VIEW FROM THE BACK-ARC APRON

The Gran Cañon Formation represents a volcaniclastic (largely pyroclastic) apron that overlapped both arc basement and ophiolitic basement (Fig. 8). The ophiolitic basement on Cedros Island was generated by rifting of arc basement (Choyal Formation) at 173 Ma (Kimbrough, 1982), and igneous activity in the arc basement continued till 163 Ma, contemporaneous with accumulation of the Gran Cañon Formation (Kimbrough, 1982; this study). Arc basement of the Choyal Formation thus represents the rear flank of a rifted arc that remained active, forming the substrate for an apron that prograded basinward with time.

Although pyroclastic aprons form only the fifth most abundant facies in modern back-arc basins of the western Pacific Ocean, they form very thick accumulations close to arcs (Klein, 1985), with high sediment accumulation rates (Karig and Moore, 1975; Macdonald and Tanner, 1983). Reported rates vary from 100–600 m/m.y. (Karig, 1971a, 1971b; Lonsdale, 1975; Cooper and others, 1979; Herman and others, 1979; Sigurdsson and others, 1980), and rates calculated for the Gran Cañon Formation (~1 km in <10 m.y.) fall in this range.

Basinward progradation of a back-arc apron with time, first predicted by Karig and Moore (1975), should result in an upward-coarsening

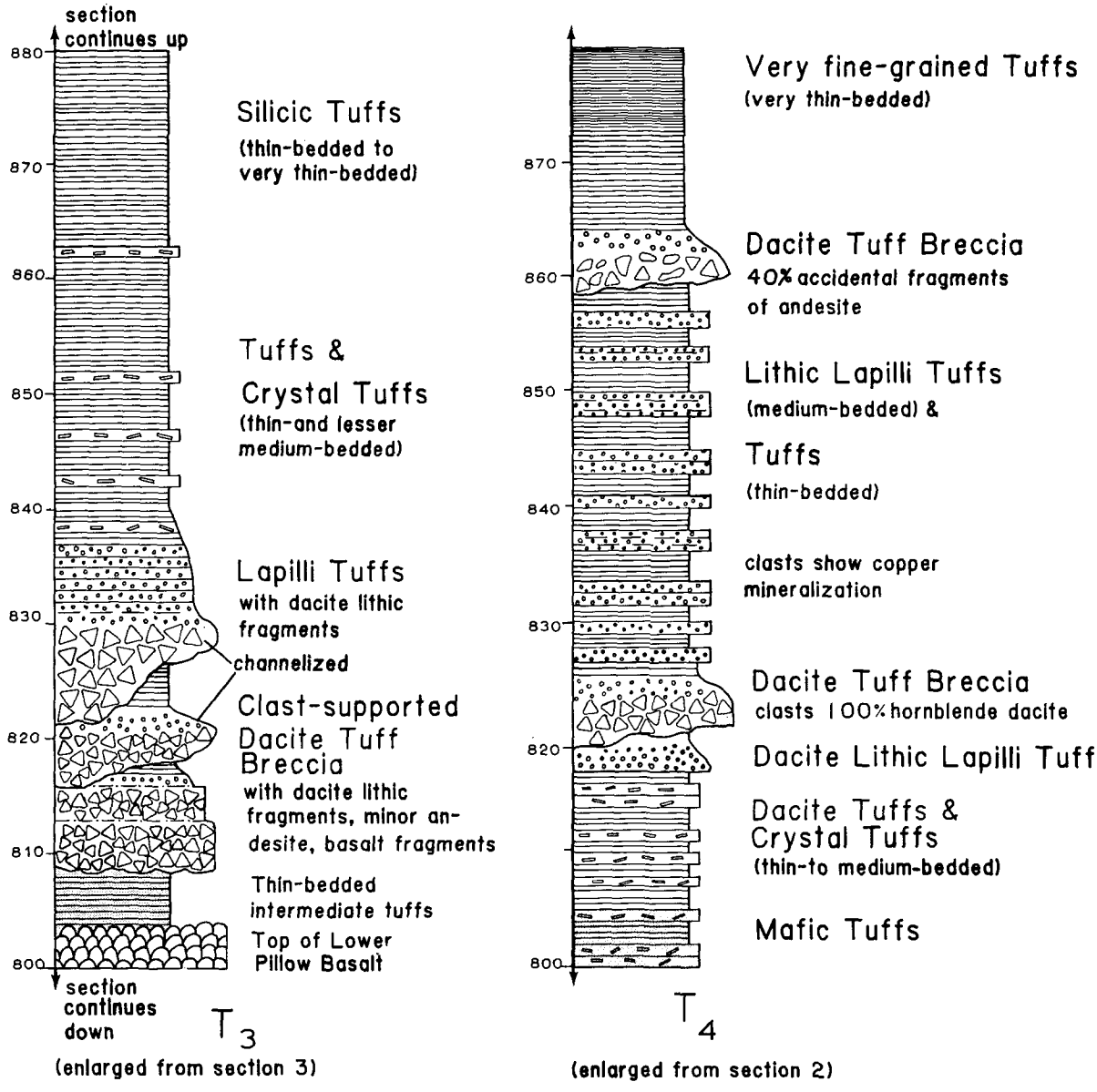

Figure 7. Measured sections through dacite pyroclastic rocks. A. Dacite pyroclastic rocks in relatively proximal parts of the back-arc apron (Arroyo Choyal area) form thick, laterally extensive horizons (see T_3 and T_4 map units of Fig. 3), with tuff breccias bearing large, nonvesiculated to poorly vesiculated juvenile lithic fragments. B. Dacite pyroclastic rocks in relatively distal parts of the back-arc apron (Arroyo Gran Cañon) have smaller lithic fragments and more pumice, and individual beds are thinner and more lenticular.

sequence of volcaniclastic sediments, such as that documented in this study (Figs. 2 and 8). Possible causes of progradation include (Mathisen and Vondra, 1983) (1) a net increase in the elevation of the arc as the volcanoes grow and, commonly, mature from island-arc tholeiites to calc-alkaline volcanic rocks, (2) subsidence of the back-arc basin, which also increases gradients to allow transport of coarse detritus farther into the basin, (3) widening of the arc by tectonic as well as magmatic processes, and (4) migration of subduction-related volcanism toward the back-arc basin with time.

The progradational back-arc apron represented by the Gran Cañon Formation records the growth and petrologic evolution of one or more adjacent arc volcanoes. In a young arc–back-arc system, at least some of the volcanoes are deeply submerged, and dispersal of ash may be relatively inefficient (Karig, 1983). The initial deposits at distances only tens of kilometres from the arc may thus be ash beds. The great thickness and relatively rapid lateral thickness variation of tuff layers in the tuff lithofacies at

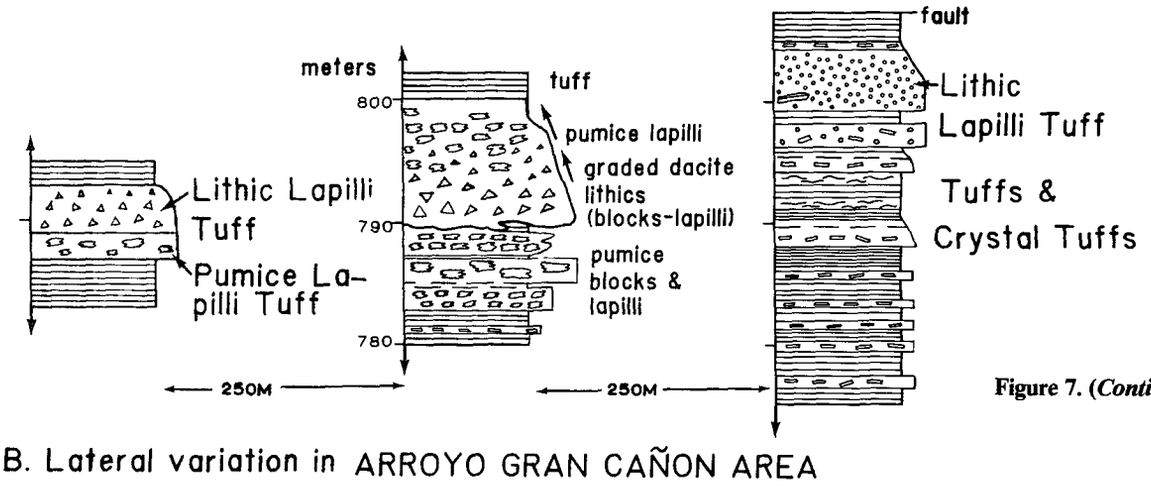

Figure 7. (*Continued*).

the base of the Gran Cañon Formation suggest that these were deposited largely from dilute, turbid flows generated by nearby deep-marine eruptions. As the summit of the adjacent volcanic edifice grew nearer to sea level, hydrostatic pressure decreased, and violent steam explosions (to form hyaloclastites) and vesiculation of magmas (to form scoria) became more common. This resulted in basinward progradation of the lapilli tuff–tuff breccia lithofacies. Blocks of shallow-water limestone were carried from the shoaling edifice to the back-arc apron by debris flows. Ultimately, abundant pyroclastic material, with pumice and bubble-wall shards, was produced during the eruption of differentiated magmas (dacites) which climaxed the growth of the adjacent volcanic edifice or arc segment (Fig. 8). Dormancy of the emergent parts of the volcanic chain, and erosion of the adjacent arc edifice with no significant tectonic uplift, resulted in blanketing of the apron with silty basinal turbidites of the epiclastic facies.

Rapid buildup of coarse detritus on proximal parts of the Gran Cañon back-arc apron resulted in development of numerous slumps, similar to those described from the Pliocene to Recent Samoan archipelagic apron (Lonsdale, 1975). The Samoan apron consists of an outer distal turbidite plain, with surface slopes less than 0°04′, and an inner bajada or proximal wedge, with surface slopes as much as 1°30′. The bajada is covered with hummocks that have amplitudes of 75 to 500 m (although smaller, undetected ones may be present). These hummocks are interpreted to be progressive slumps, where individual slide blocks move only a few metres, although the slump may propagate for tens of kilometres (Lonsdale, 1975). In the Gran Cañon Formation, coherently folded slumped intervals of block-on-block broken formation as much as 100 m thick could not have traveled far down-apron without becoming disrupted or disaggregated. Yet, debris flow deposits intimately interstratified with the slump deposits contain very large blocks of shallow-water limestone, carried all the way from the shore of the volcanic edifice. It is thus inferred that at least some of the slumps in the Gran Cañon Formation propagated along the surface of the back-arc apron from the arc region. As noted by Lonsdale (1975), of all deep-sea environments, the submarine slopes of volcanoes are especially vulnerable to sliding because of steep regional gradients (commonly in excess of 10°), high seismicity, rapid sediment accumulation, and unstable sediment structure (including the thixotropic properties of montmorillonite). Additionally, shallow-level intrusions into arc aprons on

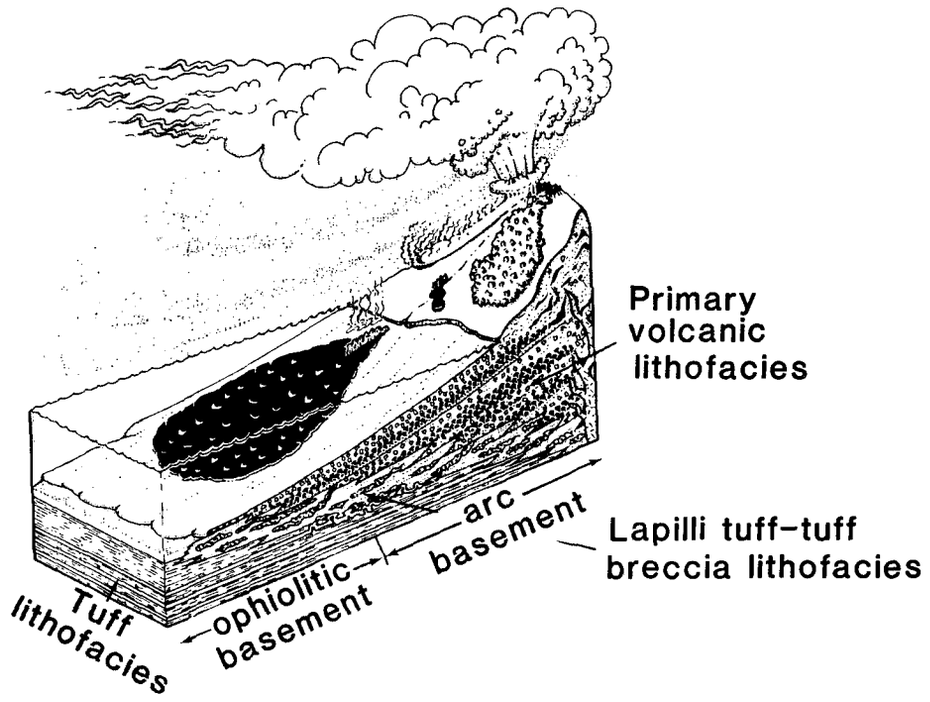

Figure 8. Paleographic reconstruction of a progradational back-arc apron, Gran Cañon Formation, Cedros Island. (Drawing by Barry R. Keller.)

steep slopes may cause sediment failure and remobilization (White and Busby-Spera, in press). The result is frequent, small, shallow slides rather than the huge, deep-seated slides of continental margins (Lonsdale, 1975). These small slides are much easier to detect in the field.

The temporal relationships between arc volcanism and rifting in back-arc basins are controversial. Scott and Kroenke (1980) proposed that volcanic maxima alternate with rifting events, whereas Karig (1983) and Klein (1985) concluded that they commonly occur coevally. Geological and geochronological evidence from Cedros Island supports the latter interpretation. The lack of pelagic sediments between the rifted arc-ophiolite basement and the overlying back-arc apron (Fig. 2), as well as the hydrothermal alteration of tuffs deposited on ophiolitic basement (Kimbrough, 1984), indicates that there was no pause in arc volcanism when rifting began. The lack of hemipelagic or epiclastic intervals within the Gran Cañon Formation, and the calculated accumulation rates, indicates continuous, rapid progradation of a pyroclastic apron into the back-arc basin, contemporaneous with the growth of an island arc.

This study of the Gran Cañon Formation on Cedros Island contributes to our knowledge of the structural and magmatic history of back-arc basins. Simple geometry of strata and lack of growth faults in the Gran Cañon back-arc apron preclude active rifting along the sides of the basin subsequent to its initiation, similar to modern back-arc aprons of the western Pacific (Karig and others, 1978). The only reported back-arc basin with active basin-wide faults is the Okinawa Trough, which formed by rifting of the Ryukyu island arc from mainland Asia (Herman and others, 1979); seafloor spreading has not yet begun in that area, however, suggesting that rifting is still in its initial stages (Weissel, 1981). It is not surprising that the frontal-arc margin of the Jurassic back-arc basin is preserved on Cedros Island, rather than the center of the basin. Many western Pacific back-arc basins have been partly subducted since their formation (Weissel, 1981), but one would expect preferential preservation of oceanic crust adjacent to the thick, less easily subducted arc massif. The "hotter" frontal-arc flank of back-arc spreading systems should be more prone to intra-plate volcanism than the "colder" remnant-arc flank (Weissel, 1981). This is consistent with the presence of laterally extensive basalt lava flows in the Gran Cañon back-arc apron, interpreted to have been fed from a fissure within the back-arc basin (Fig. 8 and Busby-Spera, in press).

SUMMARY

Detailed field, geochronological, and petrological studies of a well-preserved and well-exposed Jurassic back-arc apron in Baja California, Mexico, address fundamental questions about the evolution of arc–back-arc systems. Additionally, sedimentary structures and textures of marine pyroclastic rocks allow inference of depositional processes and construction of facies models for pyroclastic accumulations adjacent to volcanic arcs. The studies presented herein lead to the following conclusions.

I. Middle Jurassic ophiolitic rocks on Cedros Island formed in close proximity to, and contemporaneous with, island-arc igneous rocks and were immediately overlain by a section of arc-derived volcaniclastic rocks (Kimbrough, 1982, 1984; this study). The arc-ophiolite basement and the overlapping deep-marine volcaniclastic cover thus represent the frontal-arc margin of a back-arc basin. Preferential preservation of the frontal-arc margin relative to the center of a back-arc basin is predicted for ancient assemblages.

II. Back-arc apron deposits of the Gran Cañon Formation are divided into three lithofacies (in ascending order): (1) the tuff lithofacies, a basal section of tuffs deposited from turbid flows generated by deep-marine eruptions; (2) the lapilli tuff–tuff breccia lithofacies, representing resedimented hyaloclastic and scoriaceous debris. Tuff breccias of this lithofacies were deposited from nonchannelized debris flows on the proximal apron and from channelized high-density turbidity currents on distal parts of the apron; (3) the primary volcanic lithofacies, which includes monolithologic dacite pyroclastic rocks and basalt lava flows. Pumiceous dacite pyroclastic flows of low density were deposited down-apron from denser flows with unvesiculated juvenile blocks. The laterally extensive basalt flows were fed from a set of fissures that extended down the apron within the back-arc basin. Such intra-plate volcanism may be common on the "hot" frontal-arc side of back-arc basins.

III. The volcaniclastic cover of the arc-ophiolite basement, the Gran Cañon Formation, shows simple, uniform, and predictable sedimentation patterns due to (1) isolation of the basin from terrigenous sediment sources, (2) lateral and vertical differentiation of facies during progradation of pyroclastic apron into a back-arc basin, and (3) blanketing of the pyroclastic apron with volcanic lithic silts and sands eroded from the extinct arc segment within 10 m.y. of formation of the back-arc basin. This simple pattern reflects the temporal episodicity of back-arc basins and is one possible way to identify the fill of some ancient back-arc basins in orogenic zones.

IV. Progradation of back-arc aprons may directly reflect the growth and petrologic evolution of the adjacent magmatic arc, from a deeply submerged chain, with limited dispersal of ash, to a shallow-marine edifice, producing hyaloclastites and scoriaceous debris, to a high-standing arc, erupting pumiceous, differentiated magmas.

V. Slump deposits are common in the Gran Cañon back-arc apron, particularly in proximal areas, and propagate along the surface of the back-arc apron from the arc region. Slump deposits may be common features of all aprons on the flanks of volcanoes, as suggested by Lonsdale (1975).

VI. The simple geometry of the Gran Cañon Formation, like that of many modern back-arc aprons, suggests that there is no active rifting along the sides of the basin subsequent to its initiation.

VII. A blanket of silty basinal turbidites at the top of the Gran Cañon Formation records extinction and erosion, but no tectonic uplift, of the island arc. Shortly thereafter, collision of the arc–back-arc assemblage with a continental or micro-continental mass occurred (Boles and Landis, 1984), resulting in uplift of the arc and dramatic steepening of the regional paleoslope, which did not change significantly in orientation.

ACKNOWLEDGMENTS

Acknowledgment is made to the National Science Foundation (EAR-8313226 and EAR-8618771) and to the donors of the Petroleum Research Fund, administered by the American Chemical Society, for the support of this research. Special thanks are due Manuel Aguilar of Cedros Island, for arranging access to remote parts of the island. Field assistance from Barry Keller and Ellen Platzman is gratefully acknowledged. Numerous discussions with Richard V. Fisher, and reviews of this manuscript by Thomas F. Moore and Gary A. Smith, were very helpful.

REFERENCES CITED

Boles, J. R., and Landis, C. A., 1984, Jurassic sedimentary mélange and associated facies, Baja California, Mexico: Geological Society of America Bulletin, v. 95, no. 5, p. 13–21.

Bowles, F. A., Jack, R. N., and Carmichael, I.S.E., 1973, Investigation of deep-sea volcanic ash layers from equatorial Pacific cores: Geological Society of America Bulletin, v. 84, p. 2371–2388.

Busby-Spera, C. J., 1986, Depositional features of rhyolitic and andesitic volcaniclastic rocks of the Mineral King submarine caldera complex, Sierra Nevada, California: Journal of Volcanology and Geothermal Research, v. 27, p. 43–76.

——1987, Structure and organization of deep marine basalts emplaced on a volcaniclastic apron in a Middle Jurassic backarc basin, Cedros Island, Baja California, Mexico: Journal of Geology (in press).

Busby-Spera, C. J., and Keller, B., 1985, The Gran Cañon Formation: A Middle Jurassic marine volcaniclastic wedge on Cedros Island, Baja California: Geological Society of America Abstracts with Programs, v. 18, no. 2, p. 91.

Carey, S. N., and Sigurdsson, H., 1980, The Roseau Ash: Deep-sea tephra deposits from a major eruption on Dominica, Lesser Antilles arc: Journal of Volcanology and Geothermal Research, v. 7, p. 67–86.

Carlisle, D., 1963, Pillow-breccias and their aquagene tuffs, Quadra Island, British Columbia: Journal of Geology, v. 71, p. 48–71.

Cooper, A. K., Scholl, D. W., Marlow, M. S., Childs, J. R., Redden, G. D., Kvenvolden, K. A., and Stevenson, A. K., 1979, Hydrocarbon potential of Aleutian basin, Bering Sea: American Association of Petroleum Geologists Bulletin, v. 63, p. 2070–2087.

Dimroth, E., Cousineau, P., Leduc, M., and Sanchagrin, Y., 1978, Structure and organization of Archean subaqueous basalt flows, Rouyn-Noranda area, Quebec, Canada: Journal of Earth Science, v. 15, p. 902–918.

Fisher, R. V., 1964, Maximum size, median diameter, and sorting of tephra: Journal of Geophysical Research, v. 69, p. 341–355.

——1984, Submarine volcaniclastic rocks, *in* Kokelaar, B. P., and Howells, M. F., eds., Marginal basin geology—Volcanic and associated sedimentary and tectonic processes in modern and ancient basins: London, England, Blackwell Scientific Publications, p. 5–28.

Fisher, R. V., and Schmincke, H. V., 1984, Pyroclastic rocks: New York, Springer-Verlag, 472 p.

Herman, B. M., Anderson, R. N., and Truchan, M., 1979, Extensional tectonics in the Okinawa Trough, *in* Watkins, J. S., Montodert, L., and Pickerson, P. W., eds., Geological and geophysical investigation of continental margins: American Association of Petroleum Geologists Memoir 29, p. 199–208.

Hopson, C. A., Mattinson, J. M., and Pessagno, E. A., Jr., 1981, Coast Range ophiolite, western California, *in* Ernst, W. G., The geotectonic development of California (Rubey Volume I): Engelwood Cliffs, New Jersey, Prentice-Hall, p. 418–510.

Hopson, C., Beebe, W., Mattinson, J., 1986, Calif. Coast Range ophiolite: Jurassic tectonics: American Geophysical Union Abstracts with Programs (in press).

Horn, D. R., Delach, M. N., and Horn, B. M., 1969, Distribution of volcanic ash layers and turbidites in the north Pacific: Geological Society of America Bulletin, v. 81, p. 1715–1724.

Jezek, P. A., 1976, Compositional variation within and among volcanic ash layers in the Fiji Plateau area: Journal of Geology, v. 84, p. 595–616.

Jones, D. L., Blake, M. C., and Rangin, C., 1976, The four Jurassic belts of northern California and their significance to the geology of southern California borderland, *in* Howell, D. G., ed., Aspects of the California continental borderland: American Association of Petroleum Geologists, Pacific Section, Miscellaneous Publications, v. 14, p. 343–362.

Karig, D. E., 1970, Ridges and basins of the Tonga-Kermaduc island arc system: Journal of Geophysical Research, v. 75, p. 239–255.

——1971a, Structural history of the Mariana island arc system: Geological Society of America Bulletin, v. 82, p. 244–323.

——1971b, Origin and development of marginal basins in the western Pacific: Journal of Geophysical Research, v. 76, p. 2542–2561.

——1983, Temporal relationships between backarc basn formation and arc volcanism with special reference to the Philippine Sea, *in* Hayes, D. E., ed., The tectonic and geological evolution of southeast Asian seas and islands, part 2: American Geophysical Union Geophysical Monograph, v. 27, p. 318–325.

Karig, D. E., and Moore, G. F., 1975, Tectonically controlled sedimentation in marginal basins: Earth and Planetary Science Letters, v. 26, p. 233–238.

Karig, D. E., Anderson, R. N., and Bibee, L. D., 1978, Characteristics of backarc spreading in the Mariana Trough: Journal of Geophysical Research, v. 83, p. 1213–1226.

Kilmer, F. H., 1977, Reconnaissance geology of Cedros Island, Baja California, Mexico: Southern California Academy of Sciences Bulletin, v. 76, p. 91–98.

——1984, Geology of Cedros Island, Baja California, Mexico: published by Frank Kilmer, Department of Geology, Humbolt State University, Arcata, California, 69 p.

Kimbrough, D. L., 1982, Structure, petrology and geochemistry of the Mesozoic paleo-oceanic terranes of Cedros Island and the Vizcaino Peninsula, Baja California Sur, Mexico [Ph.D. thesis]: Santa Barbara, California, University of California, 395 p.

——1984, Paleogeographic significance of the Middle Jurassic Gran Cañon Formation, Cedros Island, Baja California Sur, *in* Frizzell, V. A., Jr., ed., Geology of the California Peninsula: Los Angeles, California, Pacific Section of the Society of Economic Paleontologists and Mineralogists, p. 107–118.

Klein, G. de V., 1985, The control of depositional depth, tectonic uplift, and volcanism on sedimentation processes in the backarc basins of the western Pacific: Journal of Geology, v. 93, no. 1, p. 1–25.

Klein, G. de V., and Lee, Y. T., 1984, A preliminary assessment of geodynamic controls on depositional systems and sandstone diagenesis in backarc basins, western Pacific Ocean: Tectonophysics, v. 102, p. 119–152.

Lonsdale, P. F., 1975, Sedimentation and tectonic modification of the Samoan archipelagic apron: American Association of Petroleum Geologists Bulletin, v. 59, p. 780–798.

Lowe, D. R., 1982, Sediment gravity flows: II. Depositional models with special references to the deposits of high-density turbidity currents: Journal of Sedimentary Petrology, v. 52, no. 1, p. 279–297.

Macdonald, D.I.M., and Tanner, P.W.G., 1983, Sediment dispersal patterns in part of a deformed Mesozoic backarc basin of South Georgia, South Atlantic: Journal of Sedimentary Petrology, v. 53, no. 1, p. 83–104.

Mathisen, M. E., and Vondra, C. F., 1983, The fluvial and pyroclastic deposits of the Cagayan basin, northern Luzon, Philippines—An example of non-marine volcaniclastic sedimentation in an interarc basin: Sedimentology, v. 30, p. 369–392.

Moore, J. G., and Charlton, D. W., 1984, Ultrathin lava layers exposed near San Luis Obispo Bay, California: Geology, v. 12, p. 542–545.

Ninkovich, D., Heezen, B. C., Conolly, J. R., and Burkle, L. H., 1964, South sandwich tephra in deep sea sediments: Deep-Sea Research, v. 11, p. 605–619.

Ninkovich, D., Sparks, R.S.J., and Ledbetter, M. T., 1978, The exceptional magnitude and intensity of the Toba eruption, Sumatra: An example of use of deep-sea tephra layers as a geological tool: Bulletin of Volcanology, v. 41, p. 286–298.

Saleeby, J. B., 1983, Accretionary tectonics of the North American Cordillera: Annual Review of Earth and Planetary Sciences, v. 15, p. 45–73.

Scott, R. B., and Kroenke, L. W., 1980, Evolution of backarc spreading and arc volcanism in the Philippine Sea: Interpretation of Leg 59 D.S.D.P. results, *in* Hayes, D. E., ed., The tectonic and geological evolution of southeast Asian seas and islands: American Geophysical Union Geophysical Monograph, v. 23, p. 283–291.

Self, S., and Sparks, R.S.J., 1978, Characteristics of widespread pyroclastic deposits formed by the interaction of silicic magma and water: Bulletin of Volcanology, v. 41-3, p. 1–17.

Sharp, W. D., 1980, Ophiolite accretion in the northern Sierra [abs]: EOS (American Geophysical Union Transactions), v. 61, p. 1122.

Sigurdsson, H., Sparks, R.S.J., Carey, S. N., and Huang, T. C., 1980, Volcanigenic sedimentation in the Lesser Antilles arc: Journal of Geology, v. 88, p. 523–540.

Smith, D. P., and Busby-Spera, C. J., 1987a, Fault-controlled sedimentation in a mid-Cretaceous forearc basin: Valle Formation, Cedros Island, Baja California, Mexico [abs.]: Geological Society of America, Cordilleran Section (in press).

——1987b, Petrologic trends in a mid-Cretaceous forearc basin: Valle Formation, Cedros Island, Baja California, Mexico [abs.]: American Association of Petroleum Geologists Annual Meeting (in press).

Staudigel, H., and Schmincke, H.-U., 1984, The Pliocene Seamount series of La Palma/Canary Islands: Journal of Geophysical Research, v. 89-313, p. 11195–11215.

Tanner, P.W.G., and Rex, D. C., 1979, Timing of events on a Lower Cretaceous island-arc marginal basin system on South Georgia: Geology Magazine, v. 116, p. 167–179.

Taylor, B., and Karner, G. D., 1983, On the evolution of marginal basins: Reviews of Geophysics and Space Physics, v. 21, no. 8, p. 1727–1741.

Thorarinsson, S., 1954, The eruption of Hekla 1947–48, Part 2, Chapter 3, The tephra fallout from Hekla on March 29, 1947: Societas Scientarium Islandica, Reykjavik, p. 1–68.

Walker, G.P.L., 1981, Plinian eruptions and their products: Bulletin of Volcanology, v. 44-2, p. 223–240.

Watkins, N. D., Sparks, R.S.J., Sigurdsson, H., Huang, T. C., Federman, A., Carey, S., and Ninkovich, D., 1978, Volume and extent of the Minoan tephra from Santorini: New evidence from deep sea sediment cores: Nature, p. 122–126.

Weissel, J. K., 1981, Magnetic lineations in marginal basins of the western Pacific: Royal Society of London Philosophical Transactions, ser. A, v. 300, p. 223–247.

White, J.D.L., and Busby-Spera, C. J., 1987, Deep-marine arc apron deposits and syndepositional magmatism in the Alistos Group at Punta Cono, Baja California, Mexico: Sedimentology (in press).

Williams, H., and Goles, G., 1968, Volume of the Mazama ash-fallout and the origin of Crater Lake caldera, *in* Dole, H. M., ed., Andesite conference guidebook: Oregon Department of Geology and Mineral Industries Bulletin, v. 62, p. 37–41.

Yamagishi, H., 1985, Growth of pillow lobes—Evidence from Lavas of Hokkaido, Japan, and North Island, New Zealand: Geology, v. 13, p. 499–502.

MANUSCRIPT RECEIVED BY THE SOCIETY MARCH 23, 1987
REVISED MANUSCRIPT RECEIVED AUGUST 4, 1987
MANUSCRIPT ACCEPTED AUGUST 7, 1987

Printed in U.S.A.